Influence of shot noise on phase measurement accuracy in digital holographic microscopy

Florian Charrière[1], Benjamin Rappaz[2], Jonas Kühn[1], Tristan Colomb[3], Pierre Marquet[3] and Christian Depeursinge[1]

[1]*Ecole Polytechnique Fédérale de Lausanne (EPFL), Imaging and Applied Optics Institute, CH-1015 Lausanne, Switzerland*
[2]*Ecole Polytechnique Fédérale de Lausanne (EPFL), Brain Mind Institute, CH-1015 Lausanne, Switzerland*
[3]*Centre de Neurosciences Psychiatriques, Département de psychiatrie DP-CHUV, Site de Cery, CH-1008 Prilly-Lausanne, Switzerland*
[2] *http://apl.epfl.ch/page12232.html*
Corresponding author: florian.charriere@a3.epfl.ch

Abstract: Digital Holographic Microscopy (DHM) is a single shot interferometric technique, which provides quantitative phase images with subwavelength axial accuracy. A short hologram acquisition time (down to microseconds), allows DHM to offer a reduced sensitivity to vibrations, and real time observation is achievable thanks to present performances of personal computers and charge coupled devices (CCDs). Fast dynamic imaging at low-light level involves few photons, requiring proper camera settings (integration time and gain of the CCD; power of the light source) to minimize the influence of shot noise on the hologram when the highest phase accuracy is aimed. With simulated and experimental data, a systematic analysis of the fundamental shot noise influence on phase accuracy in DHM is presented.

OCIS codes: (090.1760) Computer holography, (030.4280) Noise in imaging systems, (030.5290) Photon statistics, (120.5050) Phase measurement.

References and links

1. J. W. Goodman and R. W. Lawrence, "Digital image formation from electronically detected holograms," Appl. Phys. Lett. **11,** 77-79 (1967).
2. M.A. Kronrod, N. S. Merzlyakov, and L. P. Yaroslavskii, "Reconstruction of a hologram with a computer," Sov. Phys. Tech. Phys. **17,** 333-334 (1972).
3. E. Cuche, P. Marquet, and C. Depeursinge, "Simultaneous amplitude-contrast and quantitative phase-contrast microscopy by numerical reconstruction of Fresnel off-axis holograms," Appl. Opt. **38**, 6994-7001 (1999).
4. U. Schnars and W. P. O. Jüptner, "Digital recording and numerical reconstruction of holograms," Meas. Sci. Technol. **13,** R85-R101 (2002).
5. P. Ferraro, S. De Nicola, A. Finizio, G. Coppola, S. Grilli, C. Magro, and G. Pierattini, "Compensation of the inherent wave front curvature in digital holographic coherent microscopy for quantitative phase-contrast imaging," Appl. Opt. **42,** 1938-1946 (2003).
6. C. Liu, Z.G. Liu, F. Bo, Y. Wang, and J.Q. Zhu, "Digital holographic aberration compensation in electron holography," Opt. Eng. **42,** 651-655 (2003).
7. T. Colomb, F. Montfort, J. Kühn, N. Aspert, E. Cuche, A. Marian, F. Charrière, S. Bourquin, P. Marquet and C. Depeursinge, "Numerical parametric lens for shifting, magnification and complete aberration compensation in digital holographic microscopy," J. Opt. Soc. Am. A **23**, 3177-3190 (2006).
8. V. Kebbel, J. Muller, and W. P. O. Jüptner, "Characterization of aspherical micro-optics using digital holography: improvement of accuracy," in *Interferometry XI: Applications*, Proc. SPIE **4778**, 188-197 (2002).
9. F. Charrière, J. Kühn, T. Colomb, F. Monfort, E. Cuche, Y. Emery, K. Weible, P. Marquet, and C. Depeursinge, "Characterization of microlenses by digital holographic microscopy," Appl. Opt. **45**, 829-835 (2006).

#82596 - $15.00 USD Received 1 May 2007; revised 22 Jun 2007; accepted 22 Jun 2007; published 28 Jun 2007

10. S. Grilli, P. Ferraro, M. Paturzo, D. Alfieri, and P. De Natale, "In-situ visualization, monitoring and analysis of electric field domain reversal process in ferroelectric crystals by digital holography," Opt. Express **12**, 1832-1842 (2004).
11. G. Popescu, L. P. Deflores, J. C. Vaughan, K. Badizadegan, H. Iwai, R. R. Dasari, and M. S. Feld, "Fourier phase microscopy for investigation of biological structures and dynamics," Opt. Lett. **29**, 2503-2505 (2004).
12. B. Rappaz, P. Marquet, E. Cuche, Y. Emery, C. Depeursinge, and P. Magistretti, "Measurement of the integral refractive index and dynamic cell morphometry of living cells with digital holographic microscopy," Opt. Express **13**, 9361-9373 (2005).
13. G. N. Vishnyakov, G. G. Levin, A. V. Likhachev, V. V. Pikalov, "Phase Tomography of 3D Biological Microobjects: numerical simulation and experimental results," Opt. Spectrosc. **87**, 413-419 (1999).
14. M. K. Kim, "Tomographic three-dimensional imaging of a biological specimen using wavelength-scanning digital interference holography," Opt. Express **7,** 305-310 (2000).
15. V. Lauer, "New approach to optical diffraction tomography yielding a vector equation of diffraction tomography and a novel tomographic microscope," J. Microsc. **205**, 165–176 (2002).
16. F. Charrière, N. Pavillon, T. Colomb, Ch. Depeursinge, T. Heger, E. A.D. Mitchell, P. Marquet and B. Rappaz, "Living specimen tomography by digital holographic microscopy: morphometry of testate amoeba," Opt. Express **14**, 7005-7013 (2006).
17. T. Colomb, F. Dürr, E. Cuche, P. Marquet, H. Limberger, R.-P. Salathé, and Ch. Depeursinge, "Polarization microscopy by use of digital holography: application to optical fiber birefringence measurements," Appl. Opt. **44**, 4461-4469 (2005).
18. J. W. Goodman, *Statistical Optics* (John Wiley & Sons, New York, 1985).
19. O. Monnom, F. Dubois, C. Yourassowsky, and J. C. Legros, "Improvement in visibility of an in-focus reconstructed image in digital holography by reduction of the influence of out-of-focus objects," Appl. Opt. **44**, 3827-3832 (2005).
20. D. Paganin, A. Barty, P. J. McMahon and K. A. Nugent, "Quantitative phase-amplitude microscopy. III. The effects of noise," J. Microsc. **214**, 51-61 (2004).
21. W. J. De Ruijter and J. K. Weiss, "Detection limits in quantitative off-axis electron holography," Ultramicroscopy **50**, 269-283 (1993).
22. G. A. Mills, and I. Yamaguchi, "Effects of quantization in phase-shifting digital holography," Appl. Opt. **44**, 1216-1225 (2005).
23. T. Baumbach, E. Kolenovic, V. Kebbel, and W. Jüptner, "Improvement of accuracy in digital holography by use of multiple holograms," Appl. Opt. **45**, 6077-6085 (2006).
24. R. F. Wagner and D. G. Brown, "Unified SNR Analysis of Medical Imaging-Systems," Phys. Med. Biol. **30,** 489-518 (1985).
25. F. Charrière, T. Colomb, F. Montfort, E. Cuche, P. Marquet and Ch. Depeursinge, "Shot noise influence in reconstructed phase image SNR in digital holographic microscopy," Appl. Opt. **45**, 7667-7673 (2006).
26. G. Popescu, K. Badizadegan, R. R. Dasari, and M. S. Feld, "Observation of dynamic subdomains in red blood cells," J. Biomed. Opt. **11**, 040503-3 (2006).
27. E. Cuche, P. Marquet, and C. Depeursinge, "Aperture apodization using cubic spline interpolation: application in digital holographic microscopy," Opt. Commun. **182**, 59-69 (2000).

1. Introduction

Digital Holographic Microscopy (DHM) is a recent quantitative phase imaging technique, which is developing rapidly, offering both sub-wavelength axial accuracy and real time observation capabilities. Following the pioneer works of Goodman or Kronrod on digital holography [1-2], the method is based on the digital acquisition of a single hologram formed by an object beam passing through a microscope objective and interfering with a reference beam. The object wavefield is recovered when the hologram is re-illuminated by a digitally computed replica of the reference wave, allowing quantitative measurement of both phase and amplitude [3-4]. The transverse resolution is diffraction limited, as with classical microscopes. However, interferometric phase measurements are performed with a high precision, providing nanometric accuracy images of the optical path length through the specimen in transmission DHM, or topographic images in reflection DHM. Compared to phase-shifting interferometers, DHM offers competitive performances in terms of resolution, precision, repeatability and field of view, and has in addition three main advantages. Firstly, measurements are performed in a much shorter interval of time, as a complete measurement of the complex wavefront is obtained from a single hologram capture (down to few microseconds integration time), resulting in a reduced sensitivity to external perturbations such as vibrations. Secondly, as full measurement of the wavefront is obtained and stored digitally, DHM allows digital focusing and resulting in an extended depth of focus. Thirdly, wave front curvatures including different kind of aberrations can be numerically corrected, allowing a dramatic simplification of the optical design [5-7]. A variety of applications of this new type of optical microscopy have been described. Among others, we can mention: DHM applications in microlenses metrology [8-9]; material science [10]; live cell imaging [11-12] where DHM quantitative phase distribution contains information concerning both morphology and refractive index of the observed specimen [12]; tomography of biological specimen based on quantitative phase data acquired with DHM [13-16]; polarization and birefringence imaging [17].

In spite of the number of applications and reconstruction methods, few systematic investigations have been performed to quantify the quality and the accuracy of the reconstructed phase images. A general statistical approach was conducted by Goodman [18], but most developments were derived within the framework of speckle interferometry and are not directly applicable to the case of specimens with minimum roughness mostly investigated in DHM (polished surfaces, clean biological preparations, optical devices…). More specifically in the frame of digital holography, some studies concerning the noise reduction were proposed for specific applications: Monnom *et al.* have demonstrated an improved visibility of the reconstructed intensity images by reducing the noise due to out-of-focus objects, but the resulting amelioration is not clearly quantified and the phase behavior is not considered [19]; Paganin *et al.* investigated the effect of a uniformly distributed noise during the acquisition of the out-of-focus images required for their amplitude-based phase-retrieving algorithm; the results are however only applicable to their phase sensitive technique [20]; Ruijter and Weiss have extensively discussed the detection limit in quantitative off-axis electron holography, but their estimation of the phase variance relies principally on the fringe visibility over the hologram zone from which the phase is deduced and consequently this estimation is valid for objects with smooth phase variation only [21]; Mills and Yamaguchi have inspected the effect of the hologram quantization in phase-shifting digital holography, but have restricted their study to amplitude images [22]; Baumbach and *al.* by reducing the speckle noise in digital holography, using a proper averaging of several recorded holograms with different speckle pattern, have improved the accuracy of shape and deformation measurements [23].

In a previous paper, we proposed a general study of the signal-to-noise ratio of DHM phase images, based on the decision statistical theory proposed by Wagner and Brown [24], treating the effect of shot noise jointly with the influence of the intensity ratio between the reference and the object beams [25]. Practically, the SNR calculated within the frame of decision statistical theory helps an observer to decide if a known object is present in the noisy image or not. However despite the effect of shot noise has been discussed quantitatively, the phase accuracy in DHM images has not been addressed. Thanks to the continuous progress of personal computers and CCD, DHM is a fast growing field, particularly in the direction of dynamic measurements for life sciences [12, 26] or industrial applications. As fast dynamic imaging at low-light level involves few photons, the influence of shot noise on the hologram must be thoroughly investigated. Indeed under improper imaging conditions, it may cause a fundamental limitation in the accuracy of the reconstructed phase. Surprisingly, only few works, described in the above-mentioned references, have been reported on the subject of noise in interferometric phase measuring instruments, making difficult the definition of standard conditions for a proper comparison of the different methods performances; even commercial instruments claim performances obtained under not clearly defined measurement conditions. In this paper, for the first time to our knowledge, the influence of shot noise to the phase accuracy in DHM is clearly studied using both simulated and experimental data.

2. Material and method

2.1 Setup: the transmission DHM

The transmission DHM (Fig. 1) used for the present study has been described in details in Refs. [3] or [7]. Results presented here have been obtained with a 20x 0.4 NA microscope

#82596 - $15.00 USD Received 1 May 2007; revised 22 Jun 2007; accepted 22 Jun 2007; published 28 Jun 2007

objective. As light source, a circularized laser diode module with wavelength of 682.5 nm is used. The camera is a standard 1392 x 1040 pixels, 8 bits, black and white CCD, with a pixel size of 6.45 µm x 6.45 µm, and a maximum frame rate of 25Hz. The field of view is around 250 µm x 250 µm for a 512 x 512 pixels hologram.

The transverse resolution as well as the field of view are calibrated with the help of a USAF 1951 resolution test target. The camera comprises an electronic shutter, which enables to reduce the exposure time down to 1 µs, and an electronic gain adjustable from 0 to 25dB. With an INTEL Core 2 Duo 6600 2.4GHz, the phase image reconstruction rate described in the next chapter, reaches the value of 15 frames per second.

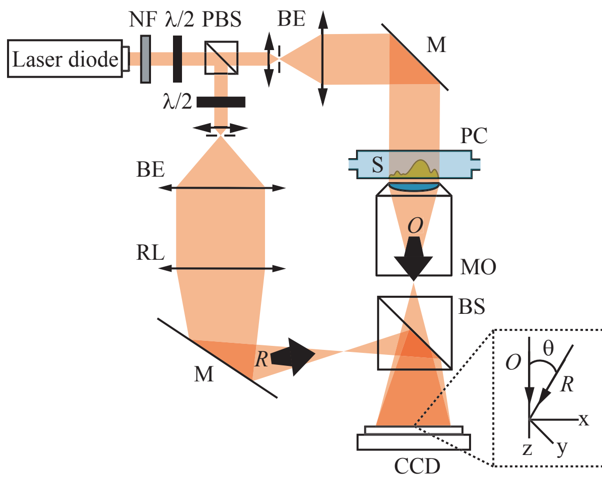

Fig. 1. Holographic microscope for transmission imaging: NF neutral density filter; PBS polarizing beam splitter; BE beam expander with spatial filter; λ/2 half-wave plate; MO microscope objective; RL field lens; M mirror; BS beam splitter; ***O*** object wave; ***R*** reference wave; PC perfusion chamber; S specimen. Inset: a detail showing the off-axis geometry at the incidence on the CCD.

2.2 Reconstruction of the holograms

The method used to process the simulated holograms is based on the convolution approach described by Schnars and Jüptner in Ref. [4] or by Colomb *et al*. in Ref. [7], where the concept of numerical lenses has been introduced to the classical formulation in order to compensate for aberrations in the optical system. As described in Ref. [7], the removal of the zero order and twin image as well as the spatial filtering are performed by applying a user-defined mask to the Fourier spectrum of the off-axis hologram. For sake of clarity, a summary of the reconstruction technique is given hereafter (see Ref. [7] for details).

The intensity distribution in the hologram plane can be described by the following expression:

$$I_H(x,y) = \underbrace{\boldsymbol{O}\boldsymbol{O}^* + \boldsymbol{R}\boldsymbol{R}^*}_{\text{zero order}} + \underbrace{\boldsymbol{O}\boldsymbol{R}^*}_{\text{real image}} + \underbrace{\boldsymbol{R}^*\boldsymbol{O}}_{\text{virtual image}} , \quad (1)$$

where $\boldsymbol{O}$ and $\boldsymbol{R}$ are respectively the interfering object and reference complex wavefront. In digital holography, the reconstruction of the wavefront $\Psi(k\Delta x, l\Delta y)$, where Δx and Δy are the pixel size of the CCD and k, l are integer values, is obtained by multiplying the hologram intensity distribution $I_H(k,l)$ with a digitally computed reference wave $\boldsymbol{R_D}(k,l)$, called the digital reference wave. Assuming a plane reference wave, $\boldsymbol{R_D}$ can be described as follows:

#82596 - $15.00 USD Received 1 May 2007; revised 22 Jun 2007; accepted 22 Jun 2007; published 28 Jun 2007

$$\boldsymbol{R_D}(k,l) = A_R \exp\left[\mathrm{i}\left(k_{Dx} \cdot k\Delta x + k_{Dy} \cdot l\Delta y \right) \right], \quad (2)$$

where k_{Dx}, and k_{Dy} are the two components of the wave vector in the hologram plane and A_R is an constant amplitude. The digitally reconstructed wave front $\Psi(k\Delta x,l\Delta y)$ is first computed in the hologram plane $x_O y_O$, and can afterward be evaluated at any distance from the hologram plane by the calculation of the scalar diffraction of the wavefront in the Fresnel approximation. $\Psi(m\Delta\xi,\ n\Delta\eta)$ is computed at a distance d from the hologram plane, in an observation plane $O\xi\eta$, by use of the following Fresnel propagation formula in the convolution formulation:

$$\Psi(m\Delta\xi, n\Delta\eta) = A\Phi(m,n) \cdot \mathrm{FFT}^{-1}\left\{ \mathrm{FFT}\left\{ \boldsymbol{R_D}(k,l) I_H\left(k,l\right)\right\}_{p,q} \cdot \exp\left[-\mathrm{i}\pi\lambda d\left(p^2+q^2\right)\right]\right\}_{m,n}, \quad (3)$$

where p,q and m,n are integers ($-N/2 \leq m,\ n < N/2$), FFT is the Fast Fourier Transform operator, FFT^{-1} is the Inverse Fast Fourier Transform operator, $A = \exp(\mathrm{i}2\pi d/\lambda)/(\mathrm{i}\lambda d)$ is a propagation constant, and $\Phi(m,n) = \exp(-\mathrm{i}\pi m^2\Delta\xi^2/(\lambda d_1) - \mathrm{i}\pi\ n^2\Delta\eta^2/(\lambda d_2))$ is the so-called digital phase mask with parameters d_1 and d_2 digitally adjusted to correct the phase aberration due to the microscope objective. $\Delta\xi=\Delta x$ and $\Delta\eta=\Delta y$ are the sampling intervals in the observation plane.

Considering only the virtual image of Eq. (1), the propagated wave front corresponding to the computed digital reference wave is:

$$\Psi = \boldsymbol{R_D}\boldsymbol{R}^*\boldsymbol{O}, \text{ with } \boldsymbol{R_D} = \exp\left[\mathrm{i}(k_{Dx} \cdot k\Delta x + k_{Dy} \cdot l\Delta y)\right], \quad (4)$$

where k_{Dx} and k_{Dy}, are two parameters adjusted to achieve identical propagation directions for $\boldsymbol{R}$ and $\boldsymbol{R_D}$.

Equation (3) requires the adjustment of four parameters for proper reconstruction of the phase distribution. The adjustment of k_{Dx} and k_{Dy} compensates for the tilt aberration resulting from the off axis geometry, while d_1 and d_2 allows to correct the wave front curvature induced by the microscope objective according to a parabolic model. Note that, in the present study, these last two parameters do not require to be adjusted in the simulated data where the curvature induced by the microscope objective was not considered. As explained in Refs. [3] or [7], the parameter values are adjusted in order to obtain a constant and homogeneous phase distribution on a flat reference surface located in or within close proximity of the specimen. The manual procedure described in Ref. [3] has been recently generalized to an automated procedure enabling the correction of optical aberrations of higher order, as described in Ref. [7].

2.3 Evaluation of the phase accuracy in the reconstructed images

As previously mentioned, there is no precise definition of the phase accuracy in absolute phase-sensitive systems, including standard interferometric systems (white-light, Mach-Zehnder, Michelson, Linnik…) or DHM. Frame averaging as well as or numerical processing of the images are commonly achieved, and basically the claimed accuracy is established for the overall procedure, while its precise characteristics including the number of samples, the total integration time, or the numerical processing methods are not specified. A definition tends nowadays to impose itself as standard: the standard spatial deviation (STD) is calculated on a defined zone of a blank phase image from which the average of 10 blank phase images has been subtracted. This way, the assumed stable phase pattern due to optics imperfections or optics misalignments is removed, allowing taking into account the temporal fluctuating noise only. Within this paper, aiming at evaluating the effect of shot noise, we have considered the STD as a measure of the phase accuracy. The cases of single-shot imaging vs temporal image averaging have been treated separately to avoid any confusion. The same analyzing procedure

#82596 - $15.00 USD Received 1 May 2007; revised 22 Jun 2007; accepted 22 Jun 2007; published 28 Jun 2007

has been applied to both the experimentally recorded and simulated holograms. First, the holograms were reconstructed according to the convolution method described above, considering a reconstruction distance d = 3 cm. The standard deviation of the phase was then calculated in a central zone of 256 x 256 pixels. The reason of evaluating the phase statistics on a restricted central zone of the reconstructed phase image, is to prevent the influence of border effects due to the discontinuity introduced by the windowing of the hologram when it is processed by both the FFT calculation and the apodization function applied to the hologram [27].

3 Holograms simulations

3.1 Principle of the simulations

Simulated holograms presented in this study have been achieved in order to theoretically determine the influence of the shot noise on the phase accuracy in DHM, either as a function of the optical power impinging the CCD or as a function of time for a given optical power. Theoretical holograms without specimen have been calculated, to determine the shot noise influence only. For all the simulations, 512 x 512 pixels holograms have been considered. All the calculations have been done in the Matlab environment. Two plane waves of equal intensities have been considered to interfere in an off-axis configuration. The calculation parameters have been adjusted according to the experimental conditions given above in the setup description: a square pixel size of 6.45 μm, a laser wavelength of 682.5 nm, and a quantification of the simulated hologram on 8 bits. The angle θ between the object and reference wave defining the off-axis configuration has been adjusted to 1.7°, with a fringes orientation of 45° with regard to the CCD vertical axis, corresponding to the experimental arrangement. After a perfect hologram has been simulated with the parameters described above, shot noise has been added, in order to simulate a realistic recorded hologram. The shot noise follows a Poisson's statistics [17], i.e. the variance of the number of photons impinging a specific pixel of the detector is equal to the mean number of photons hitting this pixel. One should remember that the shot noise depends only of the optical power, i.e. the number of photons, on the CCD, and is unavoidable in any light imaging recording process. No consideration of the other characteristics of the CCD including the full well capacity, gain linearity, readout noise or dark noise have been taken into account in the simulations, those noise sources behavior being dependent of each CCD model.

3.2 Role of the quantization of the holograms

A first simulation has been achieved in order to determine the possible role of the hologram quantization, i.e. the number of bits used to store the hologram in a digital form. The primary goal here was to establish whether an encoding on 8 bits per pixel of the simulated holograms could guarantee a sufficient accuracy or not. Consequently, a perfect hologram has been simulated with no additional noise, and stored in various format from 16 bits down to 1 bit. The spatial STD of the phase as a function of the number of bits is shown in Fig. 2(a).

#82596 - $15.00 USD Received 1 May 2007; revised 22 Jun 2007; accepted 22 Jun 2007; published 28 Jun 2007

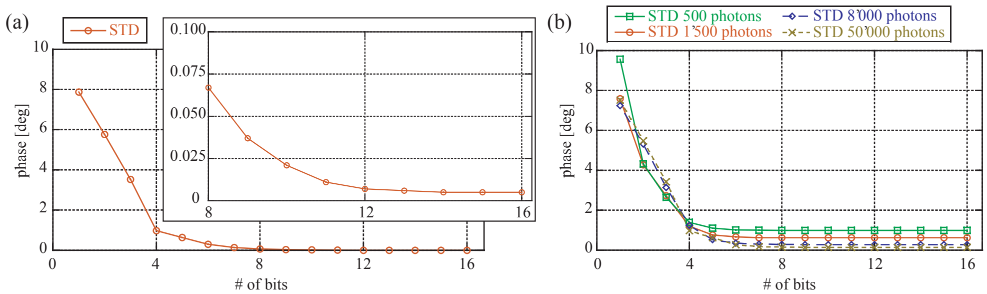

Fig. 2. Effect of hologram quantization on the standard deviation of the reconstructed phase a) for a noise-free hologram, inset exhibits a zoom on the high quantization values, and b) for a hologram with an average number of photons per pixel of 500, 1500, 8'000 and 50'000 with the corresponding shot noise.

It can be seen on Fig. 2(a), that the minimal phase STD achievable is 0.005° (λ/72'000). This minimal value is obtained for the perfect holograms encoded with 14, 15 and 16 bits, showing that the best precision of our simulation/reconstruction procedure is achieved and that accuracy can not be improved by encoding the holograms with a higher number of bits. On the other hand, the 8 bits-hologram produces a phase STD of 0.067° (λ/5'370), which far exceeds the phase STD of 0.5° corresponding to the reconstruction of a blank experimental hologram. An 8 bits storing has therefore proved to be accurate enough for both simulated and experimental data, causing no accuracy limitation during the reconstruction process.

A second simulation has been performed in order to evaluate the quantization effect on holograms with shot noise. The simulated holograms correspond to experimental holograms with an average number of photons per pixel of respectively 500, 1'500, 8'000 and 50'000. The value of 8'000 photons represents the optimal configuration available on the transmission DHM described in paragraph 2.1: with a well depth of 16ke$^-$ for the CCD pixels, an average value of 8'000 photons allows an optimal sampling of the hologram by the CCD. This configuration is achieved with an integration time of 510 µs for an irradiance on the specimen plane of few hundreds of microwatts per square centimetre, and can therefore be considered as our standard imaging conditions in transmission DHM for cells observation [11, 13]. The value of 50'000 photons corresponds to the illumination of a CCD pixel with a 100ke$^-$ full well capacity, which represents the nowadays CCDs largest full well capacity. The values of 500 and 1'500 photons were chosen to represent some non-optimal configurations available with our DHM transmission setup. In contrast, Fig. 2(b) shows that as far as noisy holograms are considered. Consequently, the phase STD as a function the number of bits presents, for values greater than 6 bits, plateaus at values depending on the simulated illumination levels only. This observation comforts us with the decision of using only an 8 bits encoding during our simulations, and demonstrates also that a quantization on 8 bits does not contribute to significantly restrict phase accuracy in our standard experimental conditions.

#82596 - $15.00 USD Received 1 May 2007; revised 22 Jun 2007; accepted 22 Jun 2007; published 28 Jun 2007

3.3 Shot noise-limited phase image accuracy

The central part of this work concerns the fundamental limitation imposed by the shot noise on the accuracy of the reconstructed phase images. The Poisson's statistic describing the photons behavior defines the unbeatable inferior limit of the phase accuracy reconstructed from on a single hologram, when a perfect detector with no additional electronic or thermal noise is considered. Results presented on Fig. 3 depict the STD in the reconstructed images as a function of the optical level, expressed through the average number of photons per pixels for simulated holograms with shot noise.

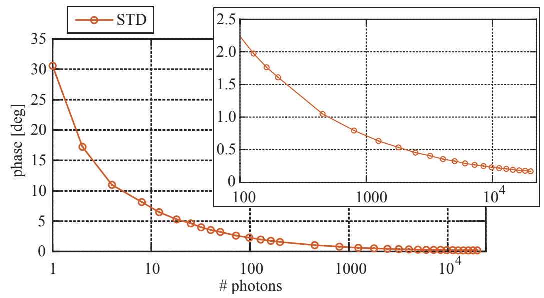

Fig. 3. Standard deviation of the phase value in the reconstructed images as a function of the optical power, expressed by the average number of photons per pixels for simulated holograms with shot noise; inset shows a zoom on the high optical power values.

This graph can be used as a simple look-up table to determine the best achievable accuracy for a given experimental configuration, knowing the integration time, the gain and the full well capacity of the CCD. For example, let us consider the optimal DHM transmission configuration used for cellular imaging in the present work: the CCD is claimed by the manufacturer to have a $16ke^-$ full well capacity; considering the power of the laser source, a maximal integration time of 510 µs can be set before saturation of the CCD, corresponding to an average number of photons per pixel of 8'000. Under this configuration, the simulated shot noise causes a phase STD of 0.25° (λ/1'440). Note that for the precedent calculations a quantum efficiency of 1 has been considered for the CCD (otherwise a simple proportionality factor exists between the number of photons impinging on a given pixel and the effective number of electrons in the well). This small example illustrates that improper imaging conditions can severely decrease the performance of a DHM setup, emphasizing the importance of the results presented on Fig. 3.

#82596 - $15.00 USD Received 1 May 2007; revised 22 Jun 2007; accepted 22 Jun 2007; published 28 Jun 2007

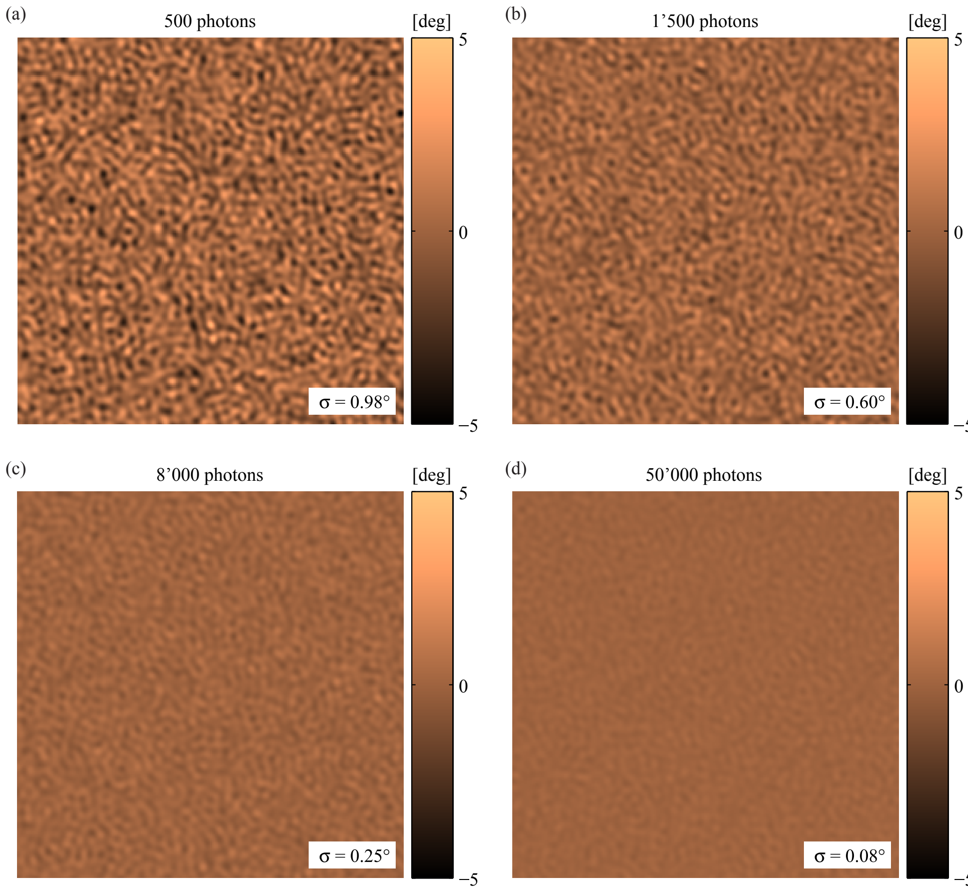

Fig. 4. Phase image (central zone of 256x256 pixels) showing the shot noise structure for simulated holograms with a mean number of photons per pixel of respectively 500 (a), 1'500 (b), 8'000 (c) and 50'000 (d); insets: the phase STD σ calculated on the phase images are indicated. A movie comprising 50 phase images illustrates the noise fluctuation [2.0 Mb].

On Fig. 4 are presented some examples of reconstructed phase images for different illumination levels: 500, 1'500, 8'000 and 50'000 mean photons per pixel. Central zones of 256x256 pixels are presented with the same color-coding scale to properly appreciate the effect of shot noise at the different illumination levels. The movie accessible from Fig. 4 allows one to appreciate the fluctuating noise in the phase images caused by shot noise. Fifty images reconstructed from simulated holograms are displayed in the movie at a rate of 6 frames per second. The observed fluctuating granular pattern has been identified to be the specific signature of shot noise. This pattern is somehow similar to a speckle pattern, with grain size corresponding to the numerical point spread function dictated by the Fresnel propagation of the algorithm used for the holograms reconstruction: the shot noise is not spatially-correlated from a pixel to another in the hologram, therefore the observed grains in the reconstructed phase image result from the addition of the numerical point spread functions multiplied by all the hologram pixels random amplitude perturbations.

In accordance with intuition, it can be seen on the graphs of Fig. 3, that the more photons involved in the hologram formation, the more accurate the reconstructed phase images. Experimentally this augmentation of the number of photons can be done in two ways: increasing the optical power of the laser source or increasing the integration time. As one of the strength of DHM is its interferometric accuracy without any insulating system, one tends to maintain a short integration time for the hologram acquisition to prevent perturbations caused by mechanical vibrations. Additionally, the power of the laser source is often fixed and can not be increased at will. Nevertheless, the number of photons can be virtually increased by performing reconstructed phase image averaging. For illustration, four series of hologram with shot noise has been simulated, with respectively an average number of photons per pixel of 500, 1’500, 8’000 (i.e. our standard experimental configuration for cellular imaging) and 50’000. On Fig. 5 are presented the STD of the reconstructed phase image as a function of the number of phase images N used in the averaging procedure. Conjointly, least-square fitted curves are also displayed on Fig. 5 with there analytical expression. It results (see Fig. 5) that, the STD as a function of the number of photons N follows almost a $N^{-1/2}$ law, except for the curve corresponding to the 50’000 mean photons: as it has be seen in the paragraph 3.2, the minimal phase STD achieved with our reconstruction procedure for a single perfect 8-bits hologram is 0.067°, what reduces the effect of averaging when the initial phase STD for a single image is already close to this minimal value, like the 0.13° obtained with 50’000 photons. This minimal noise resulting to the reconstruction algorithm also explains why decay law around $N^{-0.49}$ or $N^{-0.48}$ are observed instead of an exact $N^{-1/2}$ normally expected. This averaging technique allows for reducing the shot noise effect till the required phase accuracy is obtained. It can be seen from the graph that, for the standard case of 8’000 photons, an averaging on 10 images yields a STD of 0.08° (λ/4’500), and an averaging on 100 images allows reaching a phase STD of 0.03° (λ/12’000); at a reconstruction rate of 15 frames per second, such averaging take resp. 0.67 sec and 6.67 sec, what is somehow reasonable considering the potential gain in accuracy obtained thanks to such a procedure.

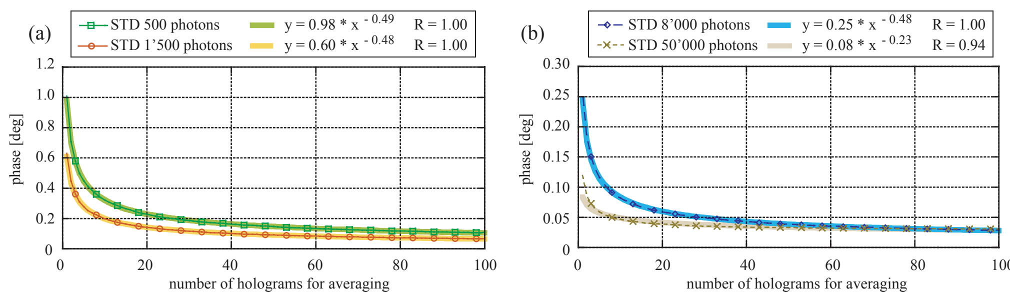

Fig. 5. Effect of averaging demonstrated on a series of simulated holograms for a mean number of photons per pixel of 1500: STD value of the reconstructed phase image as a function of the number of phase images N used in the averaging procedure with a fitted curve, which equation shows clearly the $N^{-1/2}$ tendency; R is the parameter fitter value.

4. Experimental evaluation of the shot noise in a transmission DHM

4.1 Holograms without specimen

The transmission DHM previously described was used to record holograms and confront the simulation with experimental measurements.

In a first step, a series of blank holograms was recorded, i.e. without any specimen in the system, to stress the role played by the shot noise. The maximum integration time possible in our setup before saturation of the signal was determined for no electrical gain set on the CCD. At this time value, the maximum number of photons per pixel reaches the full well capacity of $16ke^-$. To cover the largest range of intensities, we have started to record holograms with the largest shutter value, and progressively decreased it until no exploitable hologram was recordable for the given illumination level. To maintain a proper sampling of the hologram, the gain was accordingly increased to properly use the 8 bits dynamic range of the CCD. An example of phase image reconstructed from a experimentally recorded hologram with an mean number of 1’500 photons per pixel is presented on Fig. 6(a). The central zone of 256x256 pixels, on which the phase STD has been calculated, is indicated.

#82596 - \$15.00 USD Received 1 May 2007; revised 22 Jun 2007; accepted 22 Jun 2007; published 28 Jun 2007

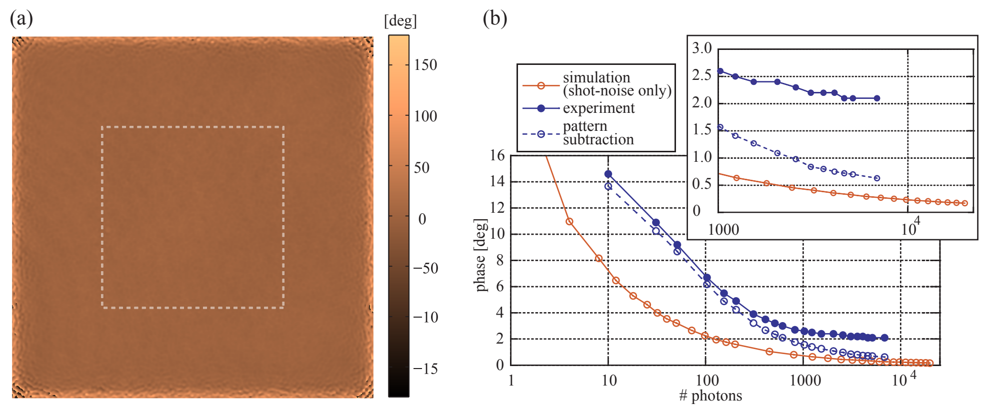

Fig. 6(a). Reconstructed phase image (512x512 pixels, field of view 250 µm x 250 µm) from an experimentally recorded blank hologram with an average photon numbers of 1'500 per pixel; the dashed zone in the image shows the 256x256 pixels square on which the phase STD was calculated. (b) Simulated (shot noise only) and experimental standard deviation of the phase in the reconstructed images as a function of the optical level, expressed as the average number of photons per pixels; the dotted curve corresponds to the experimental dataset after subtraction of the fixed phase pattern from all the reconstructed phase images; inset shows a zoom on the high optical power values.

The measured phase STD as a function of the mean number of photons per pixel is summarized on Fig. 6(b); the lower bound of the phase STD established with simulated data considering shot noise only is also displayed. The experimental values of the phase STD are larger than the shot noise limited values coming from simulation: an offset of about 2° for intensities larger than 1000 photons per pixel is observed for the experimental phase STD data compared to the simulated ones (see inset Fig. 6). This offset is caused by small defects in the setup such as non-perfect alignments of optics, imperfection of the optics surfaces, or optical aberrations. Those optical system imperfections are however stable over time, and produces a constant distortion in the phase images, manifested by a fixed phase pattern. A simple way to extract this pattern consists in averaging several images to reduce the influence of shot noise and readout noise. To verify that this pattern causes the above-mentioned offset, the experimental phase STD is recalculated, after the fixed phase pattern had been subtracted from all the reconstructed phase images. This new curve is also presented on Fig. 6(b). One can observe that this subtraction effectively removes the STD offset at higher mean intensities (above 1000 photons per pixel), showing a simple way to compensate optical imperfections of the system and thus improve its accuracy. In contrast, one observes that this subtraction has not any significant effect at lower intensities (below 100 photons per pixel). This demonstrates that the deviation of the experimental data with respect to the simulations may be explained by the imperfection of the setup for the hologram registered at higher intensities. However, another source of noise is dominating at lower intensities (electronic noise of the CCD). After subtraction of the fixed phase pattern, the averaging procedure described in chapter 3.3 has been applied to the experimental data for the case of 1500 mean photons per pixel on the hologram with a measured STD phase value of 1.34° (λ/270): the STD obtained for 10 phase images averaging is 0.5° (λ/720), going down to 0.37° (λ/830) for 30 holograms. As expected, a reduction of the phase STD is observed, but somehow less efficient as expected for a perfect $N^{-1/2}$ behavior (values resp. 15% and 25% larger than expected), what also confirms the presence of other noise source than shot noise.

Additional measurements realized with a homogeneous white light source have revealed the presence of electronic readout noise in our CCD, especially for the configurations with short integration time and strong gain. The observed readout noise appears to be structured and not uniform over the image, corresponding to the electronic architecture of the CCD itself. The structure of this noise on the CCD chip and its Fourier Transform making its

#82596 - $15.00 USD Received 1 May 2007; revised 22 Jun 2007; accepted 22 Jun 2007; published 28 Jun 2007

periodic structure clearly visible are presented on Fig. 7 for two extreme cases: a high gain with short acquisition time Fig. 7(a) and a no gain with a long acquisition time Fig. 7(b). The situation with large integration time and no gain corresponds to experimental data with high optical power of Fig. 6(b), where the experimental phase STD on reconstructed images, after subtraction of the fixed pattern noise, follows the simulated data; in this case, the readout noise can be considered sufficiently homogenous to affect negligibly the reconstructed phase images. On the other hand, the situation with large gain and short integration time corresponds to the part of the curve of Fig. 6(b), where experimental data does not follow the curve predicted by simulation (below 100 photons per pixel); in this configuration, the readout noise becomes highly structured, and affects consequently the reconstructed phase images. This noise has revealed to be sensitive to both gain and integration time, as well as to light irradiance. Therefore, the proper understanding and modeling of this readout noise is a complex and cumbersome task, which oversteps the subject of the present work focusing on the fundamental physics limitation due to shot noise, and not on the electronic handling of the CCD chip.

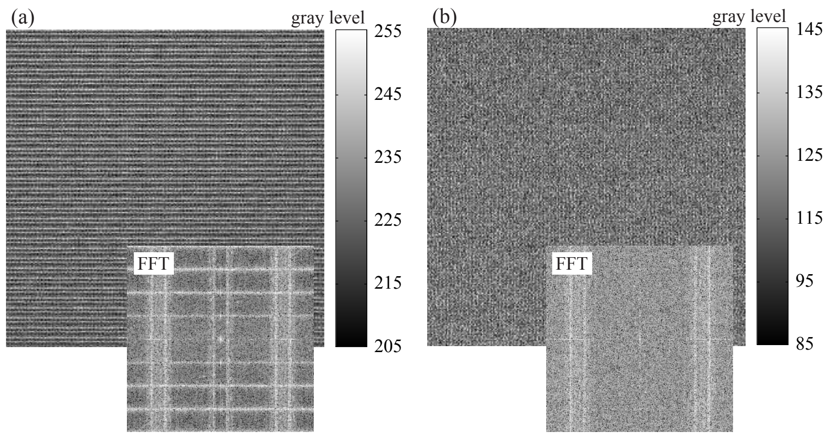

Fig. 7. Acquired frames (256x256 pixels) under homogenous illumination for extremes configurations of the CCD: (a) high gain (25dB) with short acquisition time (5µs) and (b) no gain with a long acquisition time (670 µs). For each frame, its Fourier transform is also displayed in inset.

4.2 Illustration of shot noise on living neurons phase images

In a last step, to illustrate the influence of shot noise on the phase accuracy through a practical example, we have chosen to observe 7-days old living mouse neurons in culture. The optimal case with a mean of 8'000 photons per pixel on the hologram is studied, jointly with the cases of 500 and 1'500 mean photons per pixel. Figure 8 shows the quantitative phase image of neuronal cells with their dendrites network. As depicted on the Fig. 8, the phase contrast on the cellular bodies is around 120° above the surrounding signal. It can be seen on the phase images of Fig. 8, that the signal-to-noise ratio on the cellular bodies is largely sufficient to ensure a good quality image contrast. On the other hand, as can be seen on Fig. 8, the phase signal on the neuronal network is much weaker (10 to 20 degrees). At this signal level, dynamic cell measurements as performed for example in Ref. [14], where cells morphology is investigated, or Ref. 29, where cell membranes fluctuation is studied, may become difficult in the presence of important phase fluctuations due to shot noise and would require spatial and/or temporal averaging to obtain a reliable signal, losing respectively spatial and/or temporal resolution. A comparison between Figs. 8(a), 8(b) and 8(c) allow to appreciate the reduction of the phase fluctuation caused by the shot noise in the case of incorrect versus correct imaging conditions. The cases with 500 and 1'500 mean photons per pixel have been displayed to show how the image degrade, when compared to the standard case of 8'000

#82596 - $15.00 USD Received 1 May 2007; revised 22 Jun 2007; accepted 22 Jun 2007; published 28 Jun 2007

photons, corresponding in our experimental setup to the largest integration time possible before CCD saturation, and therefore to the smallest fluctuations in single-shot phase imaging. The movie accessible from Fig. 8 presents the fluctuating noise during 50 phase images for both correct and incorrect integration time set on the CCD (parts of the phase images have been displayed on a 2x-reduced range to enhance the phase fluctuations). The results established in this work with simulations yield simple look-up tables to set the hologram acquisition parameters properly, or the number of reconstructed phase images used for averaging, to reach the targeted shot noise-limited phase accuracy in DHM required for a particular experiment.

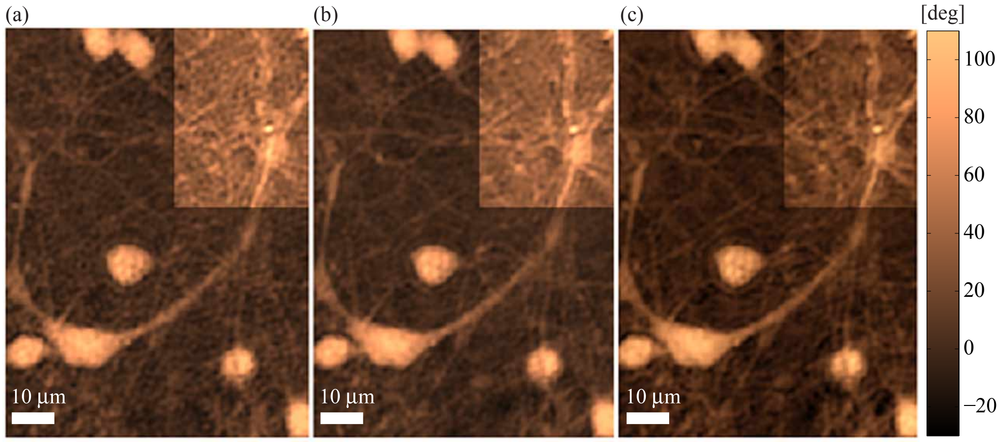

Fig. 8. Phase images (260x340 pixels) of 7-days old mouse neurons in culture, with a mean number of photons of 500 (a), 1'500 (b) and 8'000 (c): insets in images have been displayed on a 2x-reduced phase range to appreciate the reduction of the phase fluctuation caused by the shot noise in the case of non-optimal vs optimal imaging conditions. Movie [2.4Mb] presenting the fluctuating noise in (a), (b) and (c) along 50 phase images.

5. Conclusion

For the first time to our knowledge, a systematic study of the influence of shot noise on phase accuracy in DHM has been conducted. First, simulations have been used to predict the fundamental limitation due to shot noise in the case of an ideal hologram and detector. Standard deviation over the phase images as a function of the mean number of photons per pixel forming the CCD-recorded hologram have been presented, allowing one to directly estimate the phase accuracy for a DHM in an given configuration (irradiance of the source, integration time and gain of the CCD). For example, with an average number of photons of 8'000 (CCD with a 16ke$^-$ full well capacity with optimally sampled hologram), a shot noise-limited accuracy of 0.25° (λ/1'440) in the reconstructed phase images is obtained. An example has been given showing, that diminishing the integration time while keeping the same illumination level and increasing the gain to adapt the signal dynamic, a mean number of photons of 100 already deteriorates the phase accuracy by more than a factor 2, emphasizing the importance of a good comprehension of the shot noise influence on phase image accuracy, and the definition of proper imaging conditions. In a second time, the temporal averaging of a series of holograms has been studied. Practically, the expected $N^{-1/2}$ tendency, where N is the number of holograms, is observed for the STD phase value, allowing to simply reducing the effect of the shot noise as far as the desired phase accuracy is obtained. It has been showed that in the case of 8'000 mean photons per pixel, an averaging on 10 images provides a STD of 0.08° (λ/4'500), and an averaging on 100 images allows reaching a phase STD of 0.03° (λ/12'000) (averaging lasts resp. 0.67 sec and 6.67 sec at a rate of 15 frames per second). Thirdly, experimental validation of the simulations has been done with an actual DHM transmission setup, by presenting noticeably movies of the phase fluctuations induced by shot noise on mouse neuronal cells phase images. The experimental data have revealed the presence of two additional noises when compared to the simulations: for intensities lower than 1000 photons per pixel the phase accuracy is limited by the readout noise of the CCD, while for higher intensities the phase accuracy is limited by a stable phase pattern caused by the imperfections in the optical arrangement of the setup. Evidences have been presented that the readout noise of the CCD cannot be simulated easily, because it is not homogenous but spatially structured due to the electronic architecture of the CCD. This could motivate a future study dedicated to this structural noise. After subtraction from the reconstructed phase images of the stable phase pattern, the measured phase accuracy for high intensities is in good agreement with the simulations.

Acknowledgments

This work has been supported by the Swiss National Science Foundation (grant n° 205320-112195/1). The authors also would like to thank the people at Lyncée Tec SA (www.lynceetec.com), PSE-A, CH-1015 Lausanne, for their dynamism and the fructuous discussions during the paper preparation.

#82596 - $15.00 USD Received 1 May 2007; revised 22 Jun 2007; accepted 22 Jun 2007; published 28 Jun 2007